

Certifying emergent genuine multipartite entanglement with a partially blind witnessViktor Nordgren,¹ Olga Leskovjanová², Jan Provazník², Adam Johnston¹, Natalia Korolkova¹ and Ladislav Mišta, Jr.²¹*School of Physics and Astronomy, University of St. Andrews, North Haugh, St. Andrews, Fife, KY16 9SS, Scotland*²*Department of Optics, Palacký University, 17. listopadu 12, 779 00 Olomouc, Czech Republic*

(Received 28 March 2022; accepted 15 November 2022; published 9 December 2022)

Genuine multipartite entanglement underlies correlation experiments corroborating quantum mechanics and it is an expedient empowering many quantum technologies. One of many counterintuitive facets of genuine multipartite entanglement is its ability to exhibit an emergent character. That is, one can infer its presence in some multipartite states merely from a set of its separable marginals. Here we show that the effect can also be found in the context of Gaussian states of bosonic systems. Specifically, we construct examples of multimode Gaussian states carrying genuine multipartite entanglement which can be verified solely from separable nearest-neighbor two-mode marginals. The key tool of our construction is an entanglement witness acting only on some two-mode reductions of the global covariance matrix, which we find by a numerical solution of a semidefinite program. We also propose an experimental scheme for preparation of the simplest three-mode state, which requires interference of three correlatively displaced squeezed beams on two beam splitters. Besides revealing the concept of emergent genuine multipartite entanglement in the Gaussian scenario and bringing it closer to experimentally testable form, our results pave the way to effective diagnostics methods of global properties of multipartite states without complete tomography.

DOI: [10.1103/PhysRevA.106.062410](https://doi.org/10.1103/PhysRevA.106.062410)**I. INTRODUCTION**

Like from an incomplete puzzle, we assemble reality from fragments of information incoming from the outside world. This coarse-grained grasping of reality is mostly sufficient for successful and safe orientations in our environment. Barring wrong interpretation of reality, the exception to this rule may occur in situations when the partial information available to us carries no signatures of a global property, the knowledge of which is crucial for our correct decision.

There is a parallel with the quantum world here, namely, the wave function contains all available information about a state of a quantum system, but for many tasks we do not need to know it completely. However, unlike the classical world case, the fragments of the wave function may not carry traces of the global property which is important for the particular task, yet our knowledge gained from its parts can still be sufficient.

The states with that remarkable property share similarities with entangled states [1], as both exhibit a counterintuitive relationship between the whole and its parts. Not surprisingly then, states with nonlocal correlations [2,3] and, in particular, multipartite entanglement [4–9], are examples of such states, with a global property that can be inferred from parts lacking this property. Out of many flavors of multipartite entanglement [10], the main focus lies on its strongest form, the genuine multipartite entanglement, which is behind the multipartite tests of quantum nonlocality [11], complex behavior of strongly correlated systems [12], certain models of quantum computing [13], and increased precision of quantum measurements [14].

Exploration of states with genuine multipartite entanglement verifiable from separable marginals is interesting for two

reasons. First, as this sort of genuine multipartite entanglement is visible from separable marginals only, it appears as an emergent phenomenon [8] being a large-scale property of the whole, which is not present in its parts. The states that carry this kind of entanglement then can provide insight into the structure of correlations that stay behind this counterintuitive effect. The second reason is more practical, namely, the form of genuine multipartite entanglement carried by the states is subtle and thus the states may serve, similarly as bound entangled states [15], for testing as well as designation of new genuine multipartite entanglement criteria based on marginals. In fact, finding the considered states is intimately related to the development of such criteria, since one needs them for confirmation of the presence of genuine multipartite entanglement detectable from marginals. Let us emphasize that development of such economic criteria is nowadays a highly relevant topic. This is because many current applications require genuine multipartite entangled states of a large number of particles whose size makes detection of the entanglement with conventional criteria utilizing entire density matrix a difficult task. It is expected that derivation of genuine multipartite entanglement criteria working only with marginals will simplify the task significantly, similarly to what happens in the case of certification of multipartite entanglement with respect to a certain splitting based on marginals [16]. In addition, the criteria may also find applications in situations when one can for some reason access only parts of the investigated state.

Examples of quantum states, for which a global property can be inferred from the fragments lacking this property, have been discovered in the last decade only, and only for qubits [7,8]. Very recently, such qubit states that carry genuine

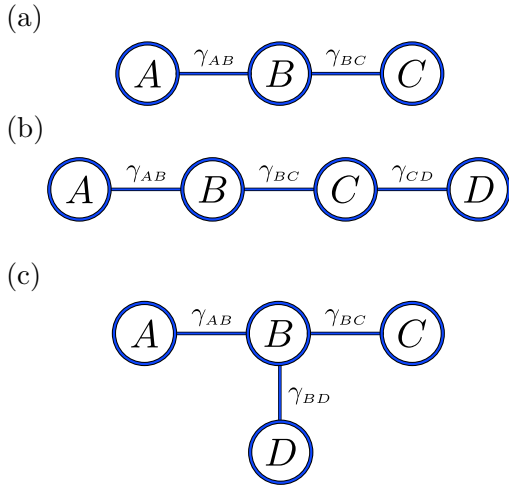


FIG. 1. Graphical representation of all minimal sets of two-mode marginals for three and four modes. The vertices represent the modes. An edge connecting modes i and j represents a two-mode marginal density matrix ρ_{ij} and it is labeled by the respective covariance matrix γ_{ij} . See text for details.

multipartite entanglement verifiable solely from separable two-qubit reduced states (marginals) were demonstrated experimentally [17]. The set of marginals used to certify the entanglement comprised *all* two-qubit marginals [7,8,17].

Interestingly, genuine multipartite entanglement can be detected even from a smaller set of separable marginals. Indeed, one can find multiqubit states that possess all two-qubit marginals separable and whose genuine multipartite entanglement can be inferred only from the so-called minimal set of two-qubit marginals [9]. The minimal set covers any part of the entire system and it contains only marginals between nearest neighbors, which guarantees that knowledge of the set suffices to confirm global entanglement. In geometric terms, if we represent parts of the global state as vertices of a graph [18] and the bipartite marginals as its edges, then the minimal set corresponds to a treelike graph. States with genuine multipartite entanglement which can be confirmed using only the elements of the minimal set were found in Ref. [9] for all configurations of up to six qubits. It has been done using the iterative numerical search algorithm [9], combining the machinery of entanglement witnesses [19,20] with the tools of semidefinite programming [21]. The best example obtained so far with qubits was a three-qubit entangled state. References [8,17] reported the lowest witness mean roughly three times smaller than the witness mean for the scenario in which all two-qubit marginals are known. Moreover, the difference is even more pronounced compared to other theoretically predicted witness means [22] of the multipartite entanglement witness experiments, already successfully implemented [23]. This indicates the complexity of the possible experimental demonstration of the studied effect using qubit states.

In this paper, we take a different approach to the problem and find the investigated property in the realm of Gaussian states [24,25]. More precisely, we look for Gaussian states with all two-mode marginals separable and whose genuine multipartite entanglement can be proved only from the minimal set of the marginals (see Fig. 1). For this purpose, we use

the methods of Gaussian multipartite entanglement witnesses [26] to assemble a Gaussian analog of the qubit search algorithm of Ref. [9]. We then find examples of the studied states for all configurations of up to six modes with the simplest examples involving only three modes, in analogy to the simplest three-qubit example [8] but with a more robust and stronger effect. The witness mean for the Gaussian three-mode genuine multipartite entanglement is roughly the same size as the theoretically predicted values [26] for some other experimentally realized Gaussian multimode entangled states [27]. Further, the required squeezing is less than one-third of a vacuum unit. Thus, the Gaussian states seem to be more promising to elucidate the specific emergent property of genuine multipartite entanglement. We devise in this paper a feasible linear-optical circuit for preparation of the three-mode state to study the effect. The scheme is based on interference of three correlatively displaced squeezed beams on three beam splitters. Our results reveal that a minimal set of overlapping separable marginals should suffice to also reveal genuine multipartite entanglement in the Gaussian scenario and indicate that Gaussian continuous variables represent a promising alternative platform for experimental demonstration of the emergent property of genuine multipartite entanglement.

II. GAUSSIAN STATES

We consider the set of Gaussian states of systems with infinite-dimensional Hilbert space, which we shall call modes in what follows. A collection of N modes A_j , $j = 1, 2, \dots, N$ can be characterized by a vector $\xi = (x_{A_1}, p_{A_1}, \dots, x_{A_N}, p_{A_N})^T$ of position and momentum quadratures x_{A_j} and p_{A_j} , respectively, which obey the canonical commutation rules $[\xi_j, \xi_k] = i(\Omega_N)_{jk}$ with $\Omega_N = \bigoplus_{j=1}^N i\sigma_y$, where σ_y is the Pauli-y matrix. Gaussian states are defined as states with a Gaussian-shaped phase-space Wigner function. An N -mode Gaussian state ρ is thus fully described by a $2N \times 1$ vector $\langle \xi \rangle = \text{Tr}[\xi \rho]$ of first moments and by a $2N \times 2N$ covariance matrix (CM) γ with entries $(\gamma)_{jk} = \langle \xi_j \xi_k + \xi_k \xi_j \rangle - 2\langle \xi_j \rangle \langle \xi_k \rangle$. The first moments can be nullified by local displacements and thus they are irrelevant as far as the correlation properties investigated here are concerned. For this reason, we set them to zero from now on.

Any CM γ reflects the uncertainty principle by satisfying the inequality

$$\gamma + i\Omega_N \geq 0, \quad (1)$$

which is not only a necessary but also a sufficient condition for a real symmetric $2N \times 2N$ matrix γ to be a CM of a physical quantum state [28]. Besides, a CM also carries complete information about the separability properties of the corresponding Gaussian state. Recall first that a quantum state ρ_{jk} of two subsystems j and k is separable if it can be expressed as a convex mixture of product states $\rho_{jk}^{\text{sep}} \equiv \sum_i p_i \rho_j^{(i)} \otimes \rho_k^{(i)}$, where $\rho_j^{(i)}$ and $\rho_k^{(i)}$ are local states of subsystems j and k , respectively. If the state cannot be written in this form, it is called entangled. Separability of a two-mode Gaussian state ρ_{jk} can be ascertained by the positive partial transposition (PPT) criterion [19,28,29]. On the CM level, the partial transposition operation \mathbb{T}_j with respect to mode j transforms the CM γ_{jk} of the state as $\gamma_{jk}^{(\mathbb{T}_j)} = (\sigma_z \oplus \mathbb{1})\gamma_{jk}(\sigma_z \oplus \mathbb{1})$, where σ_z

is the Pauli- z matrix and $\mathbb{1}$ is the 2×2 identity matrix. The PPT criterion then says [28] that the state ρ_{jk} is separable if and only if (iff) the matrix $\gamma_{jk}^{(\top j)}$ is a physical CM, i.e., iff

$$\gamma_{jk}^{(\top j)} + i\Omega_2 \geq 0. \quad (2)$$

The PPT criterion is a sufficient condition for separability only for two-mode [28] and $1 \times M$ -mode [30] Gaussian states. For systems where each party holds more than one mode, one has to use a more powerful criterion [30] according to which an N -mode Gaussian state with a CM γ consisting of an l -mode subsystem $A \equiv A_1 A_2 \dots A_l$ and an $(N - l)$ -mode subsystem $B \equiv A_{l+1} A_{l+2} \dots A_N$ is separable iff there are CMs γ_A and γ_B of the subsystems such that

$$\gamma - \gamma_A \oplus \gamma_B \geq 0. \quad (3)$$

The separability criterion (3) is advantageous because it can be formulated as the so-called semidefinite program (SDP) [21].

Recall that in its basic form an SDP is the following optimization problem [21,26]:

$$\begin{aligned} & \underset{x}{\text{minimize}} && c^\top x \\ & \text{subject to} && F(x) = F_0 + \sum_{i=1}^t F_i x_i \geq 0, \end{aligned} \quad (4)$$

which is a minimization of a real linear function $c^\top x$ of a vector $x \in \mathbb{R}^t$ under the constraint in the form of a matrix inequality $F(x) \geq 0$. The SDP (4) is specified by the vector $c \in \mathbb{R}^t$ and a set of Hermitian matrices $F_i \in \mathbb{C}^{s \times s}$, $i = 0, 1, \dots, t$, and it is commonly referred to as a primal program.

Building on these ideas, the separability criterion (3) then can be formulated as the following SDP [26]:

$$\begin{aligned} & \underset{\gamma_A, \gamma_B, x_e}{\text{minimize}} && (-x_e) \\ & \text{subject to} && \gamma - \gamma_A \oplus \gamma_B \geq 0, \\ & && \gamma_A \oplus \gamma_B + (1 + x_e)i\Omega_N \geq 0. \end{aligned} \quad (5)$$

If there is an optimal solution $x_e \geq 0$, then CM γ describes a separable state because there exist CMs γ_A and γ_B such that the separability criterion (3) is satisfied. If, on the other hand, $x_e < 0$, then the state with CM γ is entangled.

III. GAUSSIAN ENTANGLEMENT WITNESSES

In practice, one needs most often to certify the presence of entanglement in a given state rather than to show that it is separable. However, many entanglement criteria, including the PPT criterion or criterion (3), require knowledge of the entire quantum state and thus they are not economical as far as the number of measurements is concerned. This also implies that the criteria cannot be used in cases when we have access only to a part of the investigated state. Nevertheless, it is still possible to detect entanglement provided that we have some *a priori* information about the state, namely, one can prove the presence of entanglement by measuring the so-called entanglement witnesses [19,20], which requires fewer measurements compared to the measurement of the whole quantum state [31].

A. Bipartite entanglement witnesses

For a bipartite state, an entanglement witness is a Hermitian operator with a non-negative average for all separable states and a negative average on at least one entangled state. However, the task of finding entanglement witnesses for density matrices of continuous-variable modes is often hardly tractable owing to their infinite dimension. A much more simple option, which is particularly suitable for Gaussian states, is to seek entanglement witnesses for CMs [26]. For an N -mode state, such a witness is represented by a $2N \times 2N$ real, symmetric, and positive-semidefinite matrix Z , which satisfies the following conditions:

- (i) $\text{Tr}[\gamma Z] \geq 1$ for all separable γ ,
- (ii) $\text{Tr}[\gamma Z] < 1$ for some entangled γ . (6)

Entanglement detection by means of matrix Z possesses several advantages. First, the expression $\text{Tr}[\gamma Z]$ is a linear function of second moments and therefore can be measured by local homodyne detections followed by a suitable processing of the output photocurrents. More importantly, the expression also typically contains only some elements of CM γ and thus requires fewer measurements than one needs to measure the entire CM. Another advantage of using matrix Z is that for a given CM γ , it can be found numerically by solving the dual program to the program (5) [26].

Note first that the dual program to the SDP (4) is again an SDP of the following form [21]:

$$\begin{aligned} & \underset{W}{\text{maximize}} && -\text{Tr}[F_0 W] \\ & \text{subject to} && W \geq 0, \\ & && \text{Tr}[F_i W] = c_i. \end{aligned} \quad (7)$$

The importance of the dual program rests in the fact that its maximal objective value provides a lower bound on the minimal objective value of the primal program. What is more, under relatively mild assumptions the two objective values are equal [32].

By applying the generic form of the dual program (7) to the primal program (5), we get the dual program of the following form [26]:

$$\begin{aligned} & \underset{X_1, X_2}{\text{minimize}} && \text{Tr}[\gamma X_1^{\text{re}}] - 1 \\ & \text{subject to} && X_1^{\text{bd, re}} = X_2^{\text{bd, re}}, \quad X_1 \geq 0, \quad X_2 \geq 0, \\ & && \text{Tr}[i\Omega_N X_2] = -1. \end{aligned} \quad (8)$$

Here X_j ($j = 1, 2$) are $2N \times 2N$ Hermitian matrices, the symbol X_j^{re} stands for the real part of matrix X_j , and $X_j^{\text{bd}} = X_{jA} \oplus X_{jB}$, where X_{jA} and X_{jB} are diagonal blocks of matrix X_j , corresponding to subsystems A and B , respectively (bd stands for block diagonal).

It can be shown [26] that for every feasible solution $X_1 \oplus X_2$, the matrix X_1^{re} satisfies

$$\text{Tr}[\gamma X_1^{\text{re}}] \geq 1 \quad (9)$$

for every CM γ of a separable state. Further, if γ is a CM of an entangled state, then

$$\text{Tr}[\gamma X_1^{\text{re}}] < 1. \quad (10)$$

This implies that the real matrix X_1^{re} is an entanglement witness which is, in addition, optimal in the sense that it yields the minimal value of $\text{Tr}[\gamma Z]$ out of all possible witnesses Z . Needless to say, by adding more constraints into the SDP (8), one can seek witnesses with a special structure. Below we will see that one can seek witnesses which are blind to certain parts of CM γ .

B. Genuine multipartite entanglement witnesses

Bipartite entanglement is just one particular kind of entanglement. In multipartite systems consisting of $N > 2$ subsystems, one can also investigate multipartite entanglement which occurs among more than two groups of subsystems. In general, it is possible to split all subsystems into k disjoint subsets, $k \in \{N, N-1, \dots, 2\}$, and analyze entanglement with respect to this k -partite split [33]. We say that a state is k -separable with respect to a k -partite split if it can be expressed as a convex mixture of product states with respect to the split. Otherwise, the state is called as entangled with respect to the split. Since separability properties with respect to different k -partite splits are generally independent [10], a complete characterization of multipartite entanglement requires to consider all possible k -partite splits for all k . This allows us to classify multipartite states into a hierarchy of sets of states exhibiting different separability properties with respect to all the splits [10,33]. At the top of the hierarchy, there are states which are not separable with respect to any split. However, this is not the strongest form of multipartite entanglement as some of the states can be created by convex mixing of some k -separable states [34] and thus their preparation does not require interaction of all subsystems. For this reason, the concept of genuine N -partite entangled states was introduced as a synonym for states that cannot be expressed as a convex mixture of some k -separable states for any $k \geq 2$ [22]. Note that any k -separable state with $k > 2$ is also 2-separable with respect to an appropriate 2-partite split. Consequently, all states which are not genuinely N -partite entangled can then be expressed as a convex mixture of some 2-separable states, which are fittingly called biseparable states. This reveals that for the presence of genuine multipartite entanglement in a

given quantum state, it is sufficient to show that it is not biseparable.

The concept of biseparability carries over straightforwardly to CMs of N -mode Gaussian states. For this purpose, let us collect modes A_j , $j = 1, 2, \dots, N$, into the set $\mathcal{N} = \{A_1, A_2, \dots, A_N\}$ and let $\mathcal{I} = \{1, 2, \dots, N\}$ be its index set. Next, consider a nonempty proper index subset $\mathcal{J}_k = \{i_1, i_2, \dots, i_l\}$ of $0 < l < N$ elements of index set \mathcal{I} and let $\bar{\mathcal{J}}_k = \mathcal{I} \setminus \mathcal{J}_k$ denote its complement containing the remaining $N-l$ elements of \mathcal{I} . This allows us to split set \mathcal{N} into $K \equiv 2^{N-1} - 1$ different inequivalent 2-partitions, called bipartitions in what follows, $\pi(k) \equiv \mathcal{M}_{\mathcal{J}_k} | \mathcal{M}_{\bar{\mathcal{J}}_k}$, $k = 1, 2, \dots, K$, where $\mathcal{M}_{\mathcal{J}_k} = \{A_{i_1}, A_{i_2}, \dots, A_{i_l}\}$ and $\mathcal{M}_{\bar{\mathcal{J}}_k} = \mathcal{N} \setminus \mathcal{M}_{\mathcal{J}_k}$.

Moving to the criterion of biseparability, one can show [26] that an N -mode Gaussian state with CM γ is biseparable iff there exist bipartitions $\pi(k)$ and CMs $\gamma_{\pi(k)}$, which are block diagonal with respect to the bipartition $\pi(k)$, and probabilities λ_k such that

$$\gamma - \sum_{k=1}^K \lambda_k \gamma_{\pi(k)} \geq 0. \quad (11)$$

Similarly as bipartite separability can be verified by solving the SDP (5), biseparability embodied by condition (11) can also be verified by solving an SDP [26]. Analogously, just like an optimal witness of bipartite entanglement can be obtained by solving the dual problem (8) of the former SDP, the optimal witness of genuine N -partite entanglement can be found by solving the dual problem of the corresponding SDP [26]. Recall first that the witness of genuine N -partite entanglement is represented by a $2N \times 2N$ real, symmetric, and positive-semidefinite matrix Z satisfying conditions [26]

- (i) $\text{Tr}[\gamma Z] \geq 1$ for all biseparable γ ,
- (ii) $\text{Tr}[\gamma Z] < 1$ for some entangled γ . (12)

For a given CM γ , the witness can be found by solving the following dual problem [26]:

$$\begin{aligned} & \underset{X}{\text{minimize}} && \text{Tr}[\gamma X_1^{\text{re}}] - 1 \\ & \text{subject to} && X_1^{\text{re, bd, } \pi(k)} = X_{k+1}^{\text{re, bd, } \pi(k)} \quad \text{for all } k = 1, \dots, K, \\ & && \text{Tr}[i\Omega_N X_{k+1}] + X_{K+2} - X_{K+3} + X_{K+3+k} = 0, \quad \text{for all } k = 1, \dots, K, \\ & && X_{K+2} - X_{K+3} = 1. \end{aligned} \quad (13)$$

with the objective function written in its reduced form [26], Eq. (45). The minimization is performed over a Hermitian positive-semidefinite $[2N(K+1) + 2 + K]$ -dimensional block-diagonal matrix

$$X = \bigoplus_{j=1}^{2K+3} X_j, \quad (14)$$

with X_j , $j = 1, 2, \dots, K+1$ being $2N \times 2N$ Hermitian matrices and X_j , $j = K+2, K+3, \dots, 2K+3$ being 1×1 Hermitian matrices, i.e., real numbers. Only the real part of

the first component, X_1^{re} , is employed in the reduced objective function. The remaining components of X are used solely in the constraints. The k th equation $X_1^{\text{re, bd, } \pi(k)} = X_{k+1}^{\text{re, bd, } \pi(k)}$

imposes a constraint on diagonal blocks of the matrices X_1 and X_{k+1} written in the block form with respect to the bipartition $\pi(k)$. More precisely, let us express the matrix X_j in the block form with respect to the N -partite split $A_1|A_2|\dots|A_N$,

$$X_j = \begin{pmatrix} (X_j)_{11} & (X_j)_{12} & \dots & (X_j)_{1N} \\ (X_j)_{12}^\dagger & (X_j)_{22} & \dots & (X_j)_{2N} \\ \vdots & \vdots & \ddots & \vdots \\ (X_j)_{1N}^\dagger & (X_j)_{2N}^\dagger & \dots & (X_j)_{NN} \end{pmatrix}, \quad (15)$$

where $(X_j)_{mn}$ is a 2×2 block. Then the matrix $X_j^{\text{bd},\pi(k)}$ is of the same block form with the 2×2 blocks given by

$$(X_j^{\text{bd},\pi(k)})_{mn} = \begin{cases} (X_j)_{mn} & \text{if } m, n \in \mathcal{J}_k \text{ or } \bar{\mathcal{J}}_k \\ \mathbb{O} & \text{otherwise,} \end{cases} \quad (16)$$

where \mathbb{O} is the 2×2 zero matrix. For simplest cases $N = 3$ and $N = 4$, an explicit form of the matrices $X_j^{\text{bd},\pi(k)}$ can be found in Appendix A.

According to the results of Ref. [26], for every feasible solution X of the dual program (13), the matrix X_1^{re} is an optimal genuine multipartite entanglement witness.

C. Blind genuine multipartite entanglement witnesses

The witness obtained by solving the program (13) acts on the entire CM γ and therefore enables us to certify genuine multipartite entanglement provided that all elements of the CM are known. Viewed from a different perspective, it is equivalent to witnessing the entanglement from all two-mode marginal CMs because they completely determine the global CM. In this respect, the domain of Gaussian states differs from the qubit case, where the knowledge of all two-qubit marginals is not generally equivalent to the knowledge of the whole density matrix. To make the task of inference of genuine multipartite entanglement from marginals in Gaussian scenario meaningful, we thus have to work only with a proper subset of all two-mode marginal CMs. In what follows, we utilize the so-called minimal sets of bipartite marginals, which were recently introduced in Ref. [9] to solve the task for qubits. Obviously, a necessary condition for the set to allow detection of global entanglement is that it contains all modes and that one cannot divide it into a subset and its complement without having a common mode. Among all such sets, a particularly important role is played by further irreducible sets containing a minimum possible number of two-mode marginals.

A more convenient pictorial representation of such minimal sets was put forward in Ref. [9] in the form of an unlabeled tree [18], which is a special form of an undirected connected graph containing no cycles. Recall that a graph is a pair $G = (V, E)$ of a set $V = \{1, 2, \dots, N\}$ of vertices and a set $E \subseteq K \equiv \{(u, v) | (u, v) \in V^2 \wedge u \neq v\}$ of edges [35]. In our case, a vertex j of the graph represents mode A_j , whereas the edge connecting adjacent vertices j and k represents marginal CM $\gamma_{A_j A_k}$. By definition, the minimal set contains two-mode marginal CMs corresponding to the edges in the respective tree denoted as $T = (V, E')$. A closed formula for the number of nonisomorphic trees with N vertices is not known, yet for small N it can be found in Ref. [36]. In particular, all trees for the three-mode case ($N = 3$) and four-mode case

($N = 4$) are depicted in Fig. 1, where we performed the following identification: $A \equiv A_1$, $B \equiv A_2$, $C \equiv A_3$, and $D \equiv A_4$.

Ignorance of some sectors of CM γ requires us to impose some additional constraints onto the structure of the witness X_1^{re} , the solution of the SDP (13). Specifically, as the respective tree is connected, the minimal set contains all single-mode CMs as well as 2×2 blocks of correlations between the modes corresponding to the endpoints of the edges of the tree T . The part of the CM γ which we do not know is therefore given by all 2×2 off-diagonal blocks of correlations between pairs of modes carried by the marginal two-mode CMs contained in the complement of the minimal set. The elements of the complement correspond to the edges in the complement graph $\bar{T} = (V, K \setminus E')$, i.e., to the edges which have to be added to the original tree T to form the complete graph. Since for a given N the complete graph contains $\binom{N}{2}$ edges and the tree T contains exactly $N - 1$ edges [35], the number of unknown blocks of correlations is equal to $L \equiv (N - 1)(N - 2)/2$. Further, as $\text{Tr}[\gamma X_1^{\text{re}}] = \sum_{j,k} (\gamma)_{jk} (X_1^{\text{re}})_{jk}$, for the witness X_1^{re} not to act on the unknown blocks of CM γ , the blocks of X_1^{re} corresponding to the unknown blocks of γ have to vanish. More precisely, if we express the witness X_1^{re} in the block form with respect to N -partite split $A_1|A_2|\dots|A_N$ similar to Eq. (15), its 2×2 off-diagonal blocks have to satisfy the following set of L equations:

$$(X_1^{\text{re}})_{mn} = \mathbb{O} \quad \text{if } \{m, n\} \in K \setminus E', \quad (17)$$

which have to be added to the SDP (13) as additional constraints. The resulting witness X_1^{re} will thus detect genuine multipartite entanglement only from the minimal set of two-mode marginal CMs characterized by the tree T . This brings us to the following definition: A genuine multipartite entanglement witness X_1^{re} satisfying constraints (17) is called a *partially blind genuine multipartite entanglement witness corresponding to the tree T* . In particular, for $N = 3$ and the tree in Fig. 1(a), the constraint reads explicitly as

$$(X_1^{\text{re}})_{13} = \mathbb{O}. \quad (18)$$

Likewise, in the case $N = 4$ and for the linear tree in Fig. 1(b), the constraints are

$$(X_1^{\text{re}})_{13} = (X_1^{\text{re}})_{14} = (X_1^{\text{re}})_{24} = \mathbb{O}, \quad (19)$$

whereas for the t-shaped tree in Fig. 1(c), one gets the constraints of the following form:

$$(X_1^{\text{re}})_{13} = (X_1^{\text{re}})_{14} = (X_1^{\text{re}})_{34} = \mathbb{O}. \quad (20)$$

Before going further let us compare scaling of the number of independent elements of a CM needed for detection of genuine multipartite entanglement by a criterion utilizing entire CM and only minimal set of marginal CMs. Due to symmetry a generic N -mode CM containing also $x - p$ correlations possesses altogether $N(2N + 1)$ independent elements. The above graph representation allows us to calculate easily the analogous number for a given minimal set of CMs. Let us note first that to each of the N vertices of a graph representing the considered minimal set corresponds a local single-mode 2×2 CM with three independent elements. Further, to each of $N - 1$ vertices corresponds an off-diagonal 2×2 block of correlations between the modes represented by the end vertices of the edge, which has four independent elements. The

total number of independent elements is then obviously equal to $3N + 4(N - 1) = 7N - 4$. We see that while for the entire CM, the number of independent elements scales quadratically with the number of modes N , the growth is only linear for every minimal set of marginal CMs. This makes investigation of partially blind entanglement witnesses and other entanglement criteria based on minimal sets of marginals attractive because they may save a significant number of measurements, in particular, when one tests entanglement in a large multi-mode state.

IV. SEARCH ALGORITHM

The goal of the present paper is to find an example of a Gaussian state with all two-mode marginals separable and whose genuine multipartite entanglement can be verified solely from the minimal set of two-mode marginals. Recently, multiqubit examples of such states have been found [9] using a two-step algorithm proposed in Ref. [8]. Here, we employ the following Gaussian analog of the algorithm:

Step 0: Generate a random pure Gaussian state with CM γ_0 . For simplicity, we assume no $x - p$ correlations in γ_0 .

Step 1: For CM γ_0 , find a witness X_1^{re} by solving numerically the SDP (13) supplemented with the constraints (17), which we shall refer to as the SDP 1. Note, that the SDP 1 can be solved using a modification of Matlab routines provided in Ref. [26] by including the constraints (17).

Step 2: Find a CM γ that gives the least value of $\text{Tr}[\gamma X_1^{\text{re}}]$ for the witness X_1^{re} from step 1 under the constraint that the CM possesses all two-mode marginals separable. Again, the search can be accomplished by solving the following SDP:

$$\begin{aligned} & \underset{\gamma}{\text{minimize}} && \text{Tr}[\gamma X_1^{\text{re}}] \\ & \text{subject to} && \gamma + i\Omega_N \geq 0, \\ & && \gamma_{jk}^{(\text{T})} + i\Omega_2 \geq 0, \quad \text{for all } j \neq k = 1, \dots, N, \\ & && (\gamma)_{2j-1, 2k} = (\gamma)_{2j, 2k-1} = 0, \quad j, k = 1, \dots, N, \end{aligned} \quad (21)$$

which is from now on referred to as SDP 2. Here we carry out the minimization over all real symmetric $2N \times 2N$ matrices γ . The first constraint in (21) guarantees that the matrix γ is a CM of a physical quantum state, whereas the second constraint assures that all its two-mode marginal CMs γ_{jk} are separable. Finally, we perform minimization only over matrices γ which do not contain any $x - p$ correlations [the third constraint in (21) stemming from assumption in step 0].

By putting the obtained solution from step 2 as an input to step 1, we can iteratively seek the CM with the desired properties. In the next section, we use the algorithm to calculate such CMs for all configurations of up to six modes.

V. RESULTS

We did a numerical search of examples of the investigated effect for all minimal sets of marginals for up to six modes. We used MOSEK [37,38] optimization software interfaced by YALMIP [39] and PICOS [40] software libraries. By running SDP 1 and SDP 2 successively for ten iterations, for every minimal set we found many examples of CMs of states with

TABLE I. Examples of N -mode Gaussian states with all two-mode marginals separable and whose genuine multipartite entanglement can be verified from the minimal set of marginals.

N	Index	Configuration	$\text{Tr}[\gamma Z] - 1$
3	3		-14.30×10^{-2}
4	4a		-6.93×10^{-2}
	4b		-6.81×10^{-2}
5	5a		-5.71×10^{-2}
	5b		-5.17×10^{-2}
	5c		-4.14×10^{-2}
6	6a		-3.61×10^{-2}
	6b		-3.56×10^{-2}
	6c		-3.25×10^{-2}
	6d		-2.82×10^{-2}
	6e		-2.58×10^{-2}
	6f		-2.36×10^{-2}

all two-mode marginals separable and whose genuine multipartite entanglement can be verified solely from the marginals belonging to the set. The found CMs typically exhibited large diagonal entries and required high squeezing for preparation. To get experimentally easier accessible CMs, we therefore added another two constraints to SDP 2 (21). First, we limited the diagonal elements of the CM to lie within the range [1,10]. Second, we constrained the smallest eigenvalue of the sought CM γ to be above 0.2. Making use of the modified search algorithm, we then found for each configuration more than 100 examples of CMs carrying all required properties. The best examples giving the least value of $\text{Tr}[\gamma Z] - 1$ are summarized in Table I.

Similar to the qubit case [9], the absolute value of $\text{Tr}[\gamma Z] - 1$ decreases with increasing N and the trend remains preserved even if we relax the constraints on the diagonal elements and the least eigenvalue of the respective CM. However, speed at which examples of the investigated effect can be found, differs considerably in favour of the present Gaussian scenario. In the qubit case, to find a six-qubit example on a standard laptop took around 6 hours [9], whereas we needed on average less than 2 min to find an example for six modes. This can be attributed to different dimensionality of the two systems. For qubits, system size grows exponentially with the number of parties, while the growth of a size of a CM is only linear in the number of modes. The present Gaussian platform thus allows us to explore scaling of the investigated property even beyond six parties at the cost of roughly fourfold increase of the search time with addition of each mode. The largest example we found corresponded to a ten-mode linear graph,

TABLE II. Minimal eigenvalue $\varepsilon_{jk} \equiv \min\{\text{eig}[\gamma_{3,jk}^{(\top_j)} + i\Omega_2]\}$.

jk	AB	AC	BC
ε_{jk}	0.002	0.849	0.004

which gave $\text{Tr}[\gamma Z] - 1 \doteq -0.080 \times 10^{-2}$, where the symbol \doteq stands for correctly rounded to, and it took around 8 h.

In the next subsections, we provide explicit CMs of the best three-mode and four-mode examples given in the first three rows of Table I.

A. Three modes

After rounding to two decimal places, the best three-mode CM we got by running our search algorithm reads

$$\gamma_3 = \begin{pmatrix} 1.34 & 0 & -0.35 & 0 & -0.82 & 0 \\ 0 & 10.00 & 0 & 8.45 & 0 & 1.87 \\ -0.35 & 0 & 7.80 & 0 & -8.05 & 0 \\ 0 & 8.45 & 0 & 7.92 & 0 & 2.09 \\ -0.82 & 0 & -8.05 & 0 & 10.00 & 0 \\ 0 & 1.87 & 0 & 2.09 & 0 & 1.62 \end{pmatrix}.$$

By running the SDP 1 for the rounded CM γ_3 , we got $\text{Tr}[\gamma_3 Z_3] - 1 \doteq -0.143$ (see the first row in Table I). After rounding to three decimal places, the corresponding witness, blind to the correlations between a pair of modes (A, C), is given by

$$Z_3 = 10^{-2} \begin{pmatrix} 6.8 & 0 & -0.4 & 0 & 0 & 0 \\ 0 & 34.3 & 0 & -39.5 & 0 & 0 \\ -0.4 & 0 & 25.1 & 0 & 20.9 & 0 \\ 0 & -39.5 & 0 & 46.1 & 0 & -2.0 \\ 0 & 0 & 20.9 & 0 & 17.5 & 0 \\ 0 & 0 & 0 & -2.0 & 0 & 6.6 \end{pmatrix}.$$

The separability of all marginals is evidenced by Table II. Inspection of Table II reveals that all eigenvalues are strictly positive and therefore all three two-mode marginal states are separable by PPT criterion as required.

We compare now these results with the results for qubits derived in Ref. [9], benchmarking them by experimental feasi-

bility. For the simplest case of the three-mode state, we found $\text{Tr}[\gamma_3 Z_3] - 1 \doteq -0.143$. It is slightly larger than the theoretical value of -0.103 for the same quantity for Gaussian bound entanglement [26,30], a comparable effect, which was already observed experimentally [27]. For qubits, the case when all two-qubit marginals are known was recently demonstrated in Ref. [17] and the corresponding best theoretical witness mean is equal to -1.98×10^{-2} [8]. Note now that the best qubit mean of $\text{Tr}[\rho W] \doteq -6.58 \times 10^{-3}$ obtained for the three-qubit state from the minimal set [8] is approximately three times smaller than the best theoretical witness of the experimentally demonstrated case. Recall further that in the qubit scenario, the noise tolerance is 5% [8]. For comparison, the produced state with the CM $\gamma_p = \gamma_3 + p\mathbb{1}$ exhibits the effect for up to $p \doteq 0.1$ and this value is the same as for the successfully demonstrated case of Gaussian bound entanglement [26].

All these facts indicate the domain of Gaussian states is a more promising platform for the near-future experimental demonstration of the effect, and in the next section we present linear-optical setups to generate γ_3 .

B. Four modes

In the four-mode case, there are two different minimal sets of marginals corresponding to the linear tree and the t-shaped tree displayed in Figs. 1(b) and 1(c), respectively. Through the same procedure as for the three-mode case, we found CMs with the desired properties for both the minimal sets, which are given explicitly below.

1. Linear tree

First, we considered the minimal set of marginals given by the CMs γ_{AB} , γ_{BC} , and γ_{CD} , corresponding to the edges in the linear tree in Fig. 1(b). To reflect this, we included the constraints (19) into our search algorithm and produced many four-mode CMs with the desired properties. The best such CM is

$$\gamma_{4a} = \begin{pmatrix} 2.83 & 0 & -0.02 & 0 & -1.38 & 0 & 2.83 & 0 \\ 0 & 7.18 & 0 & 8.06 & 0 & 7.09 & 0 & -4.12 \\ -0.02 & 0 & 3.91 & 0 & -2.46 & 0 & 4.73 & 0 \\ 0 & 8.06 & 0 & 9.79 & 0 & 8.47 & 0 & -4.81 \\ -1.38 & 0 & -2.46 & 0 & 2.58 & 0 & -4.68 & 0 \\ 0 & 7.09 & 0 & 8.47 & 0 & 10.00 & 0 & -3.08 \\ 2.83 & 0 & 4.73 & 0 & -4.68 & 0 & 10.00 & 0 \\ 0 & -4.12 & 0 & -4.81 & 0 & -3.08 & 0 & 3.22 \end{pmatrix}. \quad (22)$$

The optimal witness Z_{4a} , which is blind to correlations of modes (A, C), (A, D), and (B, D), gives the value of $\text{Tr}[\gamma_{4a} Z_{4a}] - 1 \doteq -0.069$ (see the second row in Table I). For the expression for the witness see Appendix B. The separability of all marginals can be confirmed again by the PPT criterion (2) which is captured in Table III. As all entries in

 TABLE III. Minimal eigenvalue $\varepsilon_{jk}^{(a)} \equiv \min\{\text{eig}[\gamma_{4a,jk}^{(\top_j)} + i\Omega_2]\}$.

jk	AB	AC	AD	BC	BD	CD
$\varepsilon_{jk}^{(a)}$	0.005	0.347	0.213	0.004	0.087	0.224

TABLE IV. Minimal eigenvalue $\varepsilon_{jk}^{(b)} \equiv \min\{\text{eig}[\gamma_{4b,jk}^{(\top)} + i\Omega_2]\}$.

jk	AB	AC	AD	BC	BD	CD
$\varepsilon_{jk}^{(b)}$	0.0481	0.0032	0.5256	0.1103	0.0001	0.5489

the second row of Table III are strictly positive, all two-mode marginal CMs of CM γ_{4a} are separable as required. Note further that the effect is roughly half that of the three-mode case, which makes its experimental demonstration a bigger challenge.

2. *t-shaped tree*

Finally, we give explicitly a CM of a state whose genuine four-mode entanglement can be witnessed from its nearest-neighbor marginals as per the graph in Fig. 1(c). This corresponds to the t-shaped tree for which the minimal set comprises marginal CMs γ_{AB} , γ_{BC} , and γ_{BD} , and the witness

$$\gamma_{4b} = \begin{pmatrix} 5.23 & 0 & 0.45 & 0 & -0.02 & 0 & -2.43 & 0 \\ 0 & 1.16 & 0 & 3.00 & 0 & 1.15 & 0 & 0.51 \\ 0.45 & 0 & 3.35 & 0 & 0.91 & 0 & -5.20 & 0 \\ 0 & 3.00 & 0 & 10.00 & 0 & 3.52 & 0 & 2.06 \\ -0.02 & 0 & 0.91 & 0 & 4.09 & 0 & -2.97 & 0 \\ 0 & 1.15 & 0 & 3.52 & 0 & 1.62 & 0 & 0.62 \\ -2.43 & 0 & -5.20 & 0 & -2.97 & 0 & 10.00 & 0 \\ 0 & 0.51 & 0 & 2.06 & 0 & 0.62 & 0 & 1.49 \end{pmatrix}. \quad (23)$$

The corresponding optimal witness Z_{4b} is blind to intermodal correlations of pairs of modes (A, C) , (A, D) , and (C, D) . It gives the value of $\text{Tr}[\gamma_{4b}Z_{4b}] - 1 \doteq -0.068$ (see the third row in Table I) and its explicit form can be found in Appendix B. Once again, the separability of the marginals can be verified via the PPT criterion. The results are summarized in Table IV.

The effect is about the same strength as for the linear tree. A point to note is that, for qubits, a pure state example was found for the t-shaped tree in Ref. [9] while we found only a mixed-state example in the Gaussian scenario.

VI. EXPERIMENTAL SCHEME

In the previous section, we have seen that the investigated effect is strongest in the three-mode case. For this reason, we now derive a linear-optical scheme for the preparation of a Gaussian state with the three-mode CM γ_3 . The scheme is depicted in Fig. 2.

The scheme follows from Williamson's symplectic diagonalization of a CM [41], the Bloch-Messiah decomposition of a symplectic matrix [42], and the decomposition of an orthogonal symplectic matrix into an array of beam splitters and phase shifters [43,44]. More precisely, according to Williamson's theorem [41], for any CM γ there is a symplectic

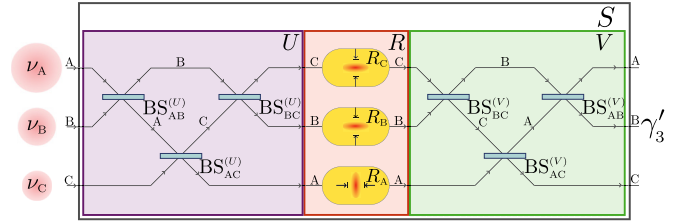


FIG. 2. Decomposition of symplectic transformation S generating a Gaussian state with CM γ_3 of three modes A, B , and C : ν_j thermal states with mean number of thermal photons $(\nu_j - 1)/2$, $j = A, B, C$ (circles); U : passive transformation consisting of beam splitters $\text{BS}_{jk}^{(U)}$, $jk = AB, AC, BC$ (leftmost box); V : passive transformation consisting of beam splitters $\text{BS}_{jk}^{(V)}$ (rightmost box); R squeezing transformation consisting of one squeezer in position quadrature, R_A , and two squeezers in momentum quadrature, R_B and R_C (middle box). For rounded parameters as in Tables V and VI, the circuit produces the CM γ'_3 , which closely approximates the CM γ_3 , and retains its entanglement properties. See text for details.

then fulfils the constraints (20). The best example CM found reads

tic transformation S which brings the CM to the normal form,

$$S\gamma S^\top = \bigoplus_{i=1}^N \nu_i \mathbb{1} \equiv \mathcal{W}, \quad (24)$$

where $\nu_1, \nu_2, \dots, \nu_N \geq 1$ are the so-called symplectic eigenvalues of CM γ . In particular, $\nu_1 = \nu_2 = \dots = \nu_N = 1$ if the state is pure. Consequently, making use of the symplectic transformation $S \equiv S^{-1}$, one can write $\gamma = S\mathcal{W}S^\top$. The symplectic eigenvalues are the magnitudes of the eigenvalues of the matrix $i\Omega\gamma$ [45] and for CM γ_3 they are written in Table V. The corresponding symplectic matrix S can be found numerically either using the method of Ref. [46] or the method of Ref. [47].

Employing the Bloch-Messiah decomposition [42], we numerically further decomposed the symplectic matrix S into

TABLE V. Symplectic eigenvalues ν_j , the squeezing parameters s_j , and the corresponding variance $V_{\text{dB}} = 10\text{Log}_{10}[(s_j)^2]$ in decibels (dB).

j	A	B	C
ν_j	6.835	1.012	1.004
s_j	0.396	0.851	0.478
V_{dB}	-8.05	-1.40	-6.41

TABLE VI. Amplitude transmissivities T_{jk} and τ_{jk} .

jk	AB	AC	BC
T_{jk}	0.555	0.947	0.492
τ_{jk}	0.716	0.904	0.657

passive transformations U and V , and an active transformation R , as

$$S = VRU. \quad (25)$$

Here, U and V are orthogonal and symplectic transformations and $R = R_A(s_A) \oplus R_B(s_B^{-1}) \oplus R_C(s_C^{-1})$ is the squeezing transformation, where $R_j(s_j) = \text{diag}(s_j, s_j^{-1})$ ($j = A, B, C$) is the diagonal matrix and the squeezing parameters $s_j < 1$ can be found in Table V. These transformations are represented by the boxes U , R , and V in Fig. 2.

Next, following the method of Refs. [43,44], one can decompose the passive transformations U and V into an array of three beam splitters as in Fig. 2,

$$\begin{aligned} U &= B_{BC}^{(U)}(T_{BC})B_{AC}^{(U)}(T_{AC})B_{AB}^{(U)}(T_{AB}), \\ V &= B_{AB}^{(V)}(\tau_{AB})B_{AC}^{(V)}(\tau_{AC})B_{BC}^{(V)}(\tau_{BC}), \end{aligned} \quad (26)$$

where the beam splitter matrices $B_{jk}^{(U)}(T_{jk})$ and $B_{jk}^{(V)}(\tau_{jk})$ ($jk = AB, AC, BC$) are given explicitly in Appendix C, and the beam splitter transmissivities T_{jk} and τ_{jk} can be found in Table VI.

Our decomposition is numerical and thus we rounded its parameters to three decimal places. Consequently, the output CM γ'_3 slightly deviates from the original CM γ_3 , yet it retains all relevant entanglement properties: it is genuinely multipartite entangled with $\text{Tr}[\gamma'_3 \bar{Z}'_3] - 1 = -0.138$ and the marginals are all separable as per Table VII. The CM γ'_3 and the corresponding witness Z'_3 can be found in Appendix D.

In the next section, we present an equivalent, yet more adapted for implementation, circuit whose output CM still retains all required properties.

A. Simplified circuit

The scheme in Fig. 2 offers two simplifications which make its experimental realization easier. First, the input states of modes B and C can be approximated by vacua (note the respective values of ν_j in Table V). Second, the classically correlated state subject to the squeezing transformations can be replaced by correlatively displaced squeezed vacuum states. This follows from the fact that a thermal state at the input of mode A can be prepared by the displacements $x_A^{(0)} \rightarrow x_A^{(0)} + t$ and $p_A^{(0)} \rightarrow p_A^{(0)} + w$ of its position and momentum vacuum quadratures $x_A^{(0)}$ and $p_A^{(0)}$, respectively. Here t and w are uncorrelated classical zero mean Gaussian random variables with

 TABLE VII. Minimal eigenvalue $\varepsilon'_{jk} \equiv \min\{\text{eig}[\gamma'_{3,jk}(\tau_{jk}) + i\Omega_2]\}$.

jk	AB	AC	BC
ε'_{jk}	0.005	0.852	0.010

 TABLE VIII. Parameters α_j and β_j of displacements (27).

j	A	B	C
α_j	0.2	-0.7	1.3
β_j	1.3	-0.5	0.3

second moments $\langle t^2 \rangle = \langle w^2 \rangle = (\nu_A - 1)/2$. On the level of quadrature operators, the transformations U and R are linear, hence we can push the displacements through the circuit and place them after the R transformation. They then attain the following form:

$$x_j \rightarrow x_j + \alpha_j t, \quad p_j \rightarrow p_j + \beta_j w, \quad j = A, B, C, \quad (27)$$

where the parameters α_j and β_j after rounding are shown in Table VIII. Further, the first step of the obtained scheme consists of application of a passive transformation U on three vacuum states, which is nothing but a triple vacuum state, and thus the transformation U can be omitted completely. In this way, we arrive at the simplified scheme depicted in Fig. 3.

Using the squeezing parameters and transmissivities found in the third row of Tables V and VI, respectively, as well as the displacements in Table VIII, the circuit in Fig. 3 produces a state which is genuinely multipartite entangled and has all marginals separable. Calling the CM of this state $\bar{\gamma}_3$, the optimal witness for this CM gives $\text{Tr}[\bar{\gamma}_3 \bar{Z}_3] - 1 = -0.139$. The numerical CM $\bar{\gamma}_3$ along with the corresponding entanglement witness may be found in Appendix D.

Verification of genuine multipartite entanglement in CM $\bar{\gamma}_3$ from marginals $\bar{\gamma}_{3,AB}$ and $\bar{\gamma}_{3,BC}$ can be carried out in two ways. One option is to measure the marginal CMs and subsequently find the respective partially blind witness by solving the SDP 1. A bigger challenge is to directly measure the witness \bar{Z}_3 . Notably, we have developed a method to find a measurement associated with a given witness, which derivation is though rather lengthy. Therefore, here we only sketch the method, whereas the details of its derivation can be found in Appendix E.

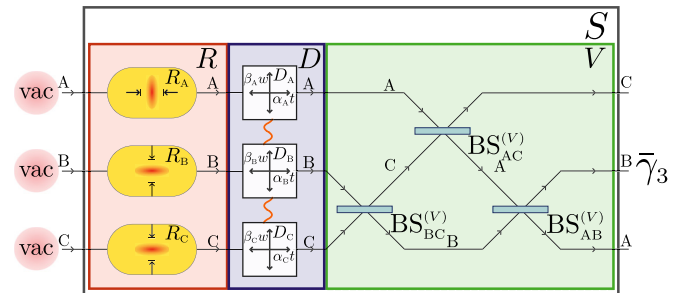


FIG. 3. Scheme for preparation of a Gaussian state with CM $\bar{\gamma}_3$ carrying genuine multipartite entanglement verifiable from nearest-neighbor separable marginals. The input comprises three vacuum states (circles). The squeezing transformation R (leftmost box) and the transformation V (rightmost box) are the same as in Fig. 2. The block D (middle box) contains correlated displacements D_A , D_B , and D_C (white boxes) given in Eq. (27), where the parameters α_j and β_j are in Table VIII and $\langle t^2 \rangle = \langle w^2 \rangle = (\nu_A - 1)/2$. See text for details.

Consider the CM $\bar{\gamma}_3$ and the witness \bar{Z}_3 , which are block diagonal with respect to the splitting into position and momentum degrees of freedom, i.e., $\bar{\gamma}_3 = \bar{\gamma}_{3x} \oplus \bar{\gamma}_{3p}$ and $\bar{Z}_3 = \bar{Z}_{3x} \oplus \bar{Z}_{3p}$, respectively. This allows us to rewrite the entanglement criterion $\text{Tr}[\bar{\gamma}_3 \bar{Z}_3] < 1$ as

$$\mathcal{U} + \mathcal{V} < \frac{1}{2}, \quad (28)$$

where $\mathcal{U} = \text{Tr}(\bar{\gamma}_{3x} \bar{Z}_{3x})/2$ and $\mathcal{V} = \text{Tr}(\bar{\gamma}_{3p} \bar{Z}_{3p})/2$. Since \bar{Z}_3 is real, symmetric, and positive-semidefinite, so are the matrices \bar{Z}_{3j} , $j = x, p$, and one can decompose them using the Cholesky decomposition as $\bar{Z}_{3j} = L_j L_j^\dagger$, where L_j is a real lower triangular matrix with nonnegative diagonal elements [48,49]. The quantities \mathcal{U} and \mathcal{V} then attain the form

$$\mathcal{U} \equiv \sum_{i=1}^3 \langle (\Delta u_i)^2 \rangle, \quad \mathcal{V} \equiv \sum_{i=1}^3 \langle (\Delta v_i)^2 \rangle, \quad (29)$$

with

$$u_i \equiv \sum_{j=1}^3 (L_x)_{ji} x_j, \quad v_i \equiv \sum_{j=1}^3 (L_p)_{ji} p_j, \quad (30)$$

where we assigned the following notation to the modes: $1 \equiv A$, $2 \equiv B$, and $3 \equiv C$. Elements of the matrices $L_{x,p}$ can be expressed in terms of elements of the matrices $(\bar{Z}_{3x,p})$ [50], Sec. 4.2.9] and hence, for the the partially blind witness \bar{Z}_3 with $(\bar{Z}_{3x,p})_{31} = 0$, we get $(L_{x,p})_{31} = 0$. We further set $(L_x)_{11} = g_1$, $(L_x)_{21} = g_2$, $(L_x)_{22} = g_3$, $(L_x)_{32} = g_4$, $(L_x)_{33} = g_5$, $(L_p)_{11} = h_1$, $(L_p)_{21} = h_2$, $(L_p)_{22} = h_3$, $(L_p)_{32} = h_4$, $(L_p)_{33} = h_5$. Then we calculate the variables (30),

$$\begin{aligned} u_1 &= g_1 x_1 + g_2 x_2, & u_2 &= g_3 x_2 + g_4 x_3, & u_3 &= g_5 x_3, \\ v_1 &= h_1 p_1 + h_2 p_2, & v_2 &= h_3 p_2 + h_4 p_3, & v_3 &= h_5 p_3, \end{aligned} \quad (31)$$

and find the quantities (29) in terms of quadrature measurements:

$$\begin{aligned} \mathcal{U} &= \langle [\Delta(g_1 x_1 + g_2 x_2)]^2 \rangle + \langle [\Delta(g_3 x_2 + g_4 x_3)]^2 \rangle \\ &\quad + g_5^2 \langle (\Delta x_3)^2 \rangle, \\ \mathcal{V} &= \langle [\Delta(h_1 p_1 + h_2 p_2)]^2 \rangle + \langle [\Delta(h_3 p_2 + h_4 p_3)]^2 \rangle \\ &\quad + h_5^2 \langle (\Delta p_3)^2 \rangle. \end{aligned} \quad (32)$$

For the witness \bar{Z}_3 , we obtain

$$\begin{aligned} \{g_1, g_2, g_3, g_4, g_5\} &= \{0.2422, -0.0224, 0.5116, 0.4107, 0.0018\}, \\ \{h_1, h_2, h_3, h_4, h_5\} &= \{0.5806, -0.6821, 0.0754, -0.2482, 0.0092\}. \end{aligned} \quad (33)$$

For the CM $\bar{\gamma}_3$ and quantities (32), this gives the values $\mathcal{U} = 0.2153$ and $\mathcal{V} = 0.2153$. As a consequence, for the CM $\bar{\gamma}_3$ the criterion (28) reads $\mathcal{U} + \mathcal{V} = 0.4306 < 1/2$. The measurement of the witness \bar{Z}_3 thus amounts to measurement of quadrature variables (31), which can be done by homodyne detection. The numerical values of the coefficients g_j and h_j are given in (33).

The simplified scheme in Fig. 3 makes experimental demonstration of the investigated effect more viable. Primarily, preparation of squeezed states at the input is easier than

implementation of squeezing operations in between beam splitter arrays U and V (compare positions of boxes R in Figs. 2 and 3). Further, the largest required amount of squeezing of -8 dB is well within the reach of the current technology [51] and can be further reduced at the cost of decreased effect strength. Additionally, the effect is immune to rounding of CMs and some parameters of the circuit components, which indicates that perfect matching of the setup parameters with the theoretical values is not critical for its demonstration. The CM $\bar{\gamma}_3$ also retains its properties under the influence of moderate losses, namely, if each of the modes is subject to the same loss characterized by the intensity transmissivity η , the resulting CM $\bar{\gamma}_{3,\eta} = \eta \bar{\gamma}_3 + (1 - \eta) \mathbb{1}$ yields $\text{Tr}[\bar{\gamma}_{3,\eta} \bar{Z}_3] - 1 < 0$ for $\eta > \eta_{\text{th}} \doteq 0.741$. Moreover, by optimizing the witness to the CM $\bar{\gamma}_{3,\eta}$, we can detect the considered effect even for higher losses of $\eta > \eta_{\text{th}}^{\text{opt}} \doteq 0.687$. Finally, as we have already mentioned, the output state tolerates the addition of a small amount of thermal noise, which is, however, of the same size as for the comparably fragile yet already demonstrated complex setup [27]. The extent to which the relatively low noise tolerance and other imperfections are detrimental to observability of the investigated phenomenon depends on the used experimental platform and will be addressed elsewhere.

VII. CONCLUSIONS

In this paper, we extended the concept of genuine multipartite entanglement verifiable from separable marginals to the domain of Gaussian states. We constructed many examples of Gaussian states possessing all two-mode marginals separable and whose genuine multipartite entanglement can be certified solely from the set of nearest-neighbor marginals. Each of the sets is characterized by a connected graph with no cycles, where the vertices represent the modes and the edges the nearest-neighbor marginals. Our examples are numerical and result from an iterative search algorithm relying on construction of a genuine multipartite entanglement witness in the space of covariance matrices. Moreover, the witness is blind to correlations between modes corresponding to nonadjacent vertices in the respective graph.

Here we gave examples for all configurations of up to six modes thus complementing the study of the investigated phenomenon in multiqubit systems [9]. Since the dimensionality of Gaussian states scales slower with the number of parties than for qubit states, we were able to also construct more complex examples involving up to ten modes.

The three-mode state we found exhibits the strongest form of the property compared to all other cases and therefore we proposed a scheme for preparation of the state, which consists of three quadrature squeezers sandwiched between two triples of phase-free beam splitters. Further, we replaced the original scheme by a simpler scheme, which still produces the desired effect but requires only interference of three squeezed states subject to correlated displacements on three beam splitters. The squeezing used in the setup is well within the reach of the current technology. Additionally, all relevant properties of the output state remain preserved under the influence of moderate losses as well as after contamination by a small amount of thermal noise, thus rendering the observation of the investigated property of genuine multipartite entanglement feasible.

A successful realization of the proposed setup would mean an extension of the experimental analysis of the phenomenon of emergent genuine multipartite entanglement [8] from qubits and the scenario when all bipartite marginals are known [17] to the realm of Gaussian states and more generic situation when only some bipartite marginals are accessible.

The impact of the presented results is multifold. First, they point at an alternative approach toward experimental investigation of the remarkable concept of genuine multipartite entanglement verifiable from incomplete sets of separable marginals, complementing experiments demonstrating Gaussian genuine multipartite entanglement by means of global inseparability criteria [52–54]. Second, here we used partially blind witnesses to construct examples of states exhibiting genuine multipartite entanglement provable from separable marginals. However, it is expected that the witnesses will also be capable of detecting genuine multipartite entanglement of many other states possessing inseparable marginals. Indeed, preliminary results indicate that all six-mode witnesses corresponding to configurations in Table I detect genuine multipartite entanglement of states prepared experimentally in Ref. [55]. Recall that in Ref. [55] multipartite entanglement with respect to all possible splits has been investigated by means of entanglement witnesses based on the separability eigenvalue equations [56] but genuine multipartite entanglement has not been analyzed. A more thorough analysis of genuine multipartite entanglement of the states of Ref. [55] using the method developed here, which would also take into account the experimental errors, is beyond the scope of the present paper and will be addressed elsewhere. Finally, the presented findings also stimulate theoretical questions concerning the existence of a Gaussian classical analog of the quantum marginal problem [57] or the extendibility of the entanglement marginal problem [16] to Gaussian case. On a more general level, our results contribute to the development of methods of detection of global properties of multipartite quantum systems from partial information.

ACKNOWLEDGMENTS

O.L. and J.P. acknowledge internal support by Palacký University through the projects IGAPrF-2021-006 and IGA-PrF-2022-005. J.P. also acknowledges support from Project No. 22-08772S of the Grant Agency of Czech Republic (GAR). J.P. further acknowledges using the computational cluster at the Department of Optics. V.N. and N.K. have been supported by the Scottish Universities Physics Alliance (SUPA) and by the Engineering and Physical Sciences Research Council (EPSRC). N.K. was supported by the EU Flagship on Quantum Technologies, project PhoG (820365).

APPENDIX A: BLOCK-DIAGONAL MATRICES IN SDP (13)

In this Appendix, we give an explicit form of matrices $X_j^{\text{bd},\pi(k)}$ appearing in SDP (13) for $N = 3$ and $N = 4$.

1. $N = 3$

For $N = 3$, we have altogether $K = 3$ bipartitions $\pi(1) = A|BC$, $\pi(2) = B|AC$ and $\pi(3) = C|AB$, where we have omit-

ted the curly brackets from the lists of elements of sets $\mathcal{M}_{\mathcal{J}_k}$ and $\bar{\mathcal{M}}_{\mathcal{J}_k}$ for brevity. The first equality in SDP (13) imposes constraints on certain elements of real parts of 6×6 Hermitian matrices X_j , $j = 1, 2, 3, 4$, which are embodied into matrices, $X_j^{\text{bd},\pi(k)}$, given explicitly as

$$\begin{aligned} X_j^{\text{bd},\pi(1)} &= \begin{pmatrix} (X_j)_{11} & \circ & \circ \\ \circ & (X_j)_{22} & (X_j)_{23} \\ \circ & (X_j)_{23}^\dagger & (X_j)_{33} \end{pmatrix}, \\ X_j^{\text{bd},\pi(2)} &= \begin{pmatrix} (X_j)_{11} & \circ & (X_j)_{13} \\ \circ & (X_j)_{22} & \circ \\ (X_j)_{13}^\dagger & \circ & (X_j)_{33} \end{pmatrix}, \\ X_j^{\text{bd},\pi(3)} &= \begin{pmatrix} (X_j)_{11} & (X_j)_{12} & \circ \\ (X_j)_{12}^\dagger & (X_j)_{22} & \circ \\ \circ & \circ & (X_j)_{33} \end{pmatrix}. \end{aligned}$$

2. $N = 4$

For $N = 4$, there are $K = 7$ bipartitions $\pi(1) = A|BCD$, $\pi(2) = B|ACD$, $\pi(3) = C|ABD$, $\pi(4) = D|ABC$, $\pi(5) = AB|CD$, $\pi(6) = AC|BD$, and $\pi(7) = AD|BC$. The matrices $X_j^{\text{bd},\pi(k)}$, $k = 1, \dots, 7$, obtained by projection of the matrices X_j onto the block-diagonal form corresponding to bipartition $\pi(k)$, read explicitly as

$$\begin{aligned} X_j^{\text{bd},\pi(1)} &= \begin{pmatrix} (X_j)_{11} & \circ & \circ & \circ \\ \circ & (X_j)_{22} & (X_j)_{23} & (X_j)_{24} \\ \circ & (X_j)_{23}^\dagger & (X_j)_{33} & (X_j)_{34} \\ \circ & (X_j)_{24}^\dagger & (X_j)_{34}^\dagger & (X_j)_{44} \end{pmatrix}, \\ X_j^{\text{bd},\pi(2)} &= \begin{pmatrix} (X_j)_{11} & \circ & (X_j)_{13} & (X_j)_{14} \\ \circ & (X_j)_{22} & \circ & \circ \\ (X_j)_{13}^\dagger & \circ & (X_j)_{33} & (X_j)_{34} \\ (X_j)_{14}^\dagger & \circ & (X_j)_{34}^\dagger & (X_j)_{44} \end{pmatrix}, \\ X_j^{\text{bd},\pi(3)} &= \begin{pmatrix} (X_j)_{11} & (X_j)_{12} & \circ & (X_j)_{14} \\ (X_j)_{12}^\dagger & (X_j)_{22} & \circ & (X_j)_{24} \\ \circ & \circ & (X_j)_{33} & \circ \\ (X_j)_{14}^\dagger & (X_j)_{24}^\dagger & \circ & (X_j)_{44} \end{pmatrix}, \\ X_j^{\text{bd},\pi(4)} &= \begin{pmatrix} (X_j)_{11} & (X_j)_{12} & (X_j)_{13} & \circ \\ (X_j)_{12}^\dagger & (X_j)_{22} & (X_j)_{23} & \circ \\ (X_j)_{13}^\dagger & (X_j)_{23}^\dagger & (X_j)_{33} & \circ \\ \circ & \circ & \circ & (X_j)_{44} \end{pmatrix}, \\ X_j^{\text{bd},\pi(5)} &= \begin{pmatrix} (X_j)_{11} & (X_j)_{12} & \circ & \circ \\ (X_j)_{12}^\dagger & (X_j)_{22} & \circ & \circ \\ \circ & \circ & (X_j)_{33} & (X_j)_{34} \\ \circ & \circ & (X_j)_{34}^\dagger & (X_j)_{44} \end{pmatrix}, \\ X_j^{\text{bd},\pi(6)} &= \begin{pmatrix} (X_j)_{11} & \circ & (X_j)_{13} & \circ \\ \circ & (X_j)_{22} & \circ & (X_j)_{24} \\ (X_j)_{13}^\dagger & \circ & (X_j)_{33} & \circ \\ \circ & (X_j)_{24}^\dagger & \circ & (X_j)_{44} \end{pmatrix}, \\ X_j^{\text{bd},\pi(7)} &= \begin{pmatrix} (X_j)_{11} & \circ & \circ & (X_j)_{14} \\ \circ & (X_j)_{22} & (X_j)_{23} & \circ \\ \circ & (X_j)_{23}^\dagger & (X_j)_{33} & \circ \\ (X_j)_{14}^\dagger & \circ & \circ & (X_j)_{44} \end{pmatrix}. \end{aligned}$$

APPENDIX B: FOUR-MODE NUMERICAL EXAMPLES

We give an explicit form of numeric witnesses for the four-mode CMs γ_{4a} and γ_{4b} detecting genuine multipartite entanglement from minimal sets of two-mode marginal CMs characterized by the linear tree and the t-shaped tree in Figs. 1(b) and 1(c), respectively.

1. Linear tree

The witness which detects the genuine multipartite entanglement of CM γ_{4a} without accessing correlations between pairs of modes (A, C) , (A, D) , and (B, D) is

$$Z_{4a} = 10^{-2} \cdot \begin{pmatrix} 2.70 & 0 & -1.12 & 0 & 0 & 0 & 0 & 0 \\ 0 & 33.29 & 0 & -28.67 & 0 & 0 & 0 & 0 \\ -1.12 & 0 & 6.86 & 0 & 6.30 & 0 & 0 & 0 \\ 0 & -28.67 & 0 & 29.50 & 0 & -5.46 & 0 & 0 \\ 0 & 0 & 6.30 & 0 & 74.73 & 0 & 33.42 & 0 \\ 0 & 0 & 0 & -5.46 & 0 & 7.37 & 0 & 2.18 \\ 0 & 0 & 0 & 0 & 33.42 & 0 & 16.30 & 0 \\ 0 & 0 & 0 & 0 & 0 & 2.18 & 0 & 4.11 \end{pmatrix}.$$

2. t-shaped tree

The witness detecting genuine multipartite entanglement of CM γ_{4b} , which is blind with respect to correlations between the pairs of modes (A, C) , (A, D) , (C, D) , reads

$$Z_{4b} = 10^{-2} \begin{pmatrix} 1.9945 & 0 & -0.8208 & 0 & 0 & 0 & 0 & 0 \\ 0 & 75.6563 & 0 & -25.8998 & 0 & 0 & 0 & 0 \\ -0.8208 & 0 & 38.01 & 0 & -1.5390 & 0 & 19.7516 & 0 \\ 0 & -25.8998 & 0 & 17.9417 & 0 & -21.9613 & 0 & -0.7569 \\ 0 & 0 & -1.5390 & 0 & 2.9227 & 0 & 0 & 0 \\ 0 & 0 & 0 & -21.9613 & 0 & 54.329 & 0 & 0 \\ 0 & 0 & 19.7516 & 0 & 0 & 0 & 10.5835 & 0 \\ 0 & 0 & 0 & -0.7569 & 0 & 0 & 0 & 3.1455 \end{pmatrix}.$$

APPENDIX C: BEAM SPLITTER TRANSFORMATIONS

In this Appendix, we give explicit form of beam splitter matrices appearing in Eq. (26) of the main text,

$$B_{AB}^{(U)}(T_{AB}) = \begin{pmatrix} T_{AB}\mathbb{1} & R_{AB}\mathbb{1} & \mathbb{O} \\ R_{AB}\mathbb{1} & -T_{AB}\mathbb{1} & \mathbb{O} \\ \mathbb{O} & \mathbb{O} & -1 \end{pmatrix},$$

$$B_{AC}^{(U)}(T_{AC}) = \begin{pmatrix} T_{AC}\mathbb{1} & \mathbb{O} & R_{AC}\mathbb{1} \\ \mathbb{O} & 1 & \mathbb{O} \\ R_{AC}\mathbb{1} & \mathbb{O} & -T_{AC}\mathbb{1} \end{pmatrix},$$

$$B_{BC}^{(U)}(T_{BC}) = \begin{pmatrix} 1 & \mathbb{O} & \mathbb{O} \\ \mathbb{O} & -T_{BC}\mathbb{1} & -R_{BC}\mathbb{1} \\ \mathbb{O} & R_{BC}\mathbb{1} & -T_{BC}\mathbb{1} \end{pmatrix},$$

$$B_{AB}^{(V)}(\tau_{AB}) = \begin{pmatrix} \tau_{AB}\mathbb{1} & \rho_{AB}\mathbb{1} & \mathbb{O} \\ \rho_{AB}\mathbb{1} & -\tau_{AB}\mathbb{1} & \mathbb{O} \\ \mathbb{O} & \mathbb{O} & 1 \end{pmatrix},$$

$$B_{AC}^{(V)}(\tau_{AC}) = \begin{pmatrix} -\tau_{AC}\mathbb{1} & \mathbb{O} & \rho_{AC}\mathbb{1} \\ \mathbb{O} & 1 & \mathbb{O} \\ -\rho_{AC}\mathbb{1} & \mathbb{O} & -\tau_{AC}\mathbb{1} \end{pmatrix},$$

$$B_{BC}^{(V)}(\tau_{BC}) = \begin{pmatrix} 1 & \mathbb{O} & \mathbb{O} \\ \mathbb{O} & \tau_{BC}\mathbb{1} & \rho_{BC}\mathbb{1} \\ \mathbb{O} & \rho_{BC}\mathbb{1} & -\tau_{BC}\mathbb{1} \end{pmatrix},$$

where the transmissivities T_{jk} and τ_{jk} are given in Table VI of the main text, while $R_{jk} = \sqrt{1 - T_{jk}^2}$ and $\rho_{jk} = \sqrt{1 - \tau_{jk}^2}$ are the corresponding reflectivities.

APPENDIX D: CIRCUIT OUTPUT COVARIANCE MATRICES

In this Appendix, we present output CMs, witnesses, and relevant eigenvalues of linear-optical circuits in Figs. 2 and 3.

1. Circuit in Fig. 2

First, we present the results for the scheme in Fig. 2 with parameters given in Tables V and VI of the main text. In this case the output CM, rounded to two decimal places, is given by

$$\gamma_3' = \begin{pmatrix} 1.34 & 0 & -0.35 & 0 & -0.82 & 0 \\ 0 & 10.01 & 0 & 8.45 & 0 & 1.86 \\ -0.35 & 0 & 7.78 & 0 & -8.03 & 0 \\ 0 & 8.45 & 0 & 7.92 & 0 & 2.08 \\ -0.82 & 0 & -8.03 & 0 & 9.99 & 0 \\ 0 & 1.86 & 0 & 2.08 & 0 & 1.62 \end{pmatrix}.$$

The corresponding witness then reads

$$Z'_3 = 10^{-2} \begin{pmatrix} 6.856 & 0 & -0.453 & 0 & 0 & 0 \\ 0 & 34.115 & 0 & -39.307 & 0 & 0 \\ -0.453 & 0 & 25.035 & 0 & 20.874 & 0 \\ 0 & -39.307 & 0 & 45.925 & 0 & -2.051 \\ 0 & 0 & 20.874 & 0 & 17.426 & 0 \\ 0 & 0 & 0 & -2.051 & 0 & 6.622 \end{pmatrix}$$

and it gives $\text{Tr}[\gamma'_3 Z'_3] - 1 = -0.138$.

Further, the marginals of the CMs are all separable, as can be seen in Table IX.

2. Circuit in Fig. 3

In this section, we derive and analyze entanglement properties of the CM $\bar{\gamma}_3$ at the output of the circuit in Fig. 3.

Initially, vacuum modes A , B , and C enter quadrature squeezers with squeezing parameters given in the second row of Table V. Next, they are subject to displacements

$$x_j \rightarrow x_j + \alpha_j t, \quad p_j \rightarrow p_j + \beta_j w, \quad (\text{D1})$$

where t and w are zero mean Gaussian random variables with second moments $\langle t^2 \rangle = \langle w^2 \rangle = (v_A - 1)/2$ and where the parameters α_j and β_j are given in Table VIII. Finally, the three modes interfere on an array of three beam splitters described by the matrix V in Eq. (26). At the output of the circuit, one gets the following CM:

$$\bar{\gamma}_3 = \begin{pmatrix} 1.39 & 0 & -0.21 & 0 & -1.05 & 0 \\ 0 & 9.95 & 0 & 8.26 & 0 & 1.7 \\ -0.21 & 0 & 7.36 & 0 & -7.83 & 0 \\ 0 & 8.26 & 0 & 7.63 & 0 & 1.94 \\ -1.05 & 0 & -7.83 & 0 & 10.12 & 0 \\ 0 & 1.7 & 0 & 1.94 & 0 & 1.59 \end{pmatrix}. \quad (\text{D2})$$

The optimal witness, which gives $\text{Tr}[\bar{\gamma}_3 \bar{Z}_3] - 1 = -0.139$, is given by

$$\bar{Z}_3 = 10^{-2} \begin{pmatrix} 5.867 & 0 & -0.543 & 0 & 0 & 0 \\ 0 & 33.707 & 0 & -39.602 & 0 & 0 \\ -0.543 & 0 & 26.222 & 0 & 21.009 & 0 \\ 0 & -39.602 & 0 & 47.097 & 0 & -1.872 \\ 0 & 0 & 21.009 & 0 & 16.865 & 0 \\ 0 & 0 & 0 & -1.872 & 0 & 6.167 \end{pmatrix}. \quad (\text{D3})$$

All marginals are separable as evidenced by Table X.

APPENDIX E: WITNESS MEASUREMENT

In the last Appendix, we show how to decompose a generic N -mode entanglement witness Z into local quadrature measurements. In particular, we give explicitly the measurement for the witness \bar{Z}_3 , Eq. (D3), detecting genuine multipartite entanglement of the state at the output of the circuit in Fig. 3 from the minimal set of two-mode marginals.

Consider N modes labeled by indexes $1, 2, \dots, N$. Let us start with an observation that for CMs without $x - p$ correlations, which are considered in this paper, we can assume without loss of any generality the witness matrix Z in the same form [26], Proposition 3. More precisely, if we re-

order the vector of quadratures ξ as $\tilde{\xi} = (\xi_x^\top, \xi_p^\top)^\top$, where $\xi_x = (x_1, x_2, \dots, x_N)^\top$ and $\xi_p = (p_1, p_2, \dots, p_N)^\top$, the CMs analyzed by us are of the block-diagonal form $\gamma = \gamma_x \oplus \gamma_p$ and the corresponding witness then can be assumed to be also block diagonal, $Z = Z_x \oplus Z_p$. Consequently, we can rewrite the entanglement criterion (12) [26] as

$$\text{Tr}(\gamma Z) = \text{Tr}(\gamma_x Z_x) + \text{Tr}(\gamma_p Z_p) < 1. \quad (\text{E1})$$

Next, the matrices Z are always real, symmetric, and positive-semidefinite and so are blocks Z_x and Z_p . This allows us to apply the Cholesky decomposition to each block and express it as $Z_j = L_j L_j^\top$, where L_j is a real lower triangular matrix with nonnegative diagonal elements [48,49]. If the blocks Z_j are positive definite the matrix L_j is, in addition, unique, nonsingular and possesses strictly positive diago-

TABLE IX. Minimal eigenvalue $\varepsilon'_{jk} \equiv \min\{\text{eig}[\gamma_{3,jk}^{(\top_j)} + i\Omega_2]\}$.

jk	AB	AC	BC
ε'_{jk}	0.005	0.852	0.010

TABLE X. Minimal eigenvalue $\bar{\varepsilon}_{jk} \equiv \min\{\text{eig}[\bar{\gamma}_{3,jk}^{(\top_j)} + i\Omega_2]\}$.

jk	AB	AC	BC
$\bar{\varepsilon}_{jk}$	0.027	0.862	0.037

nal elements [48], Corollary 7.2.9]. In a generic case of positive-semidefinite blocks Z_j , the Cholesky decomposition still exists, but some diagonal elements of the matrix L_j can be equal to zero and the matrix need not be unique [49], p. 8.3]. Making use of the Cholesky decomposition, the cyclic property of the matrix trace and the definition of a CM, we then get

$$\begin{aligned} \text{Tr}(\gamma_j Z_j) &= \text{Tr}(\gamma_j L_j L_j^\top) = \sum_{i=1}^N (L_j^\top \gamma_j L_j)_{ii} \\ &= 2 \sum_{i=1}^N \langle [\Delta(L_j^\top \xi_j)_i]^2 \rangle, \end{aligned} \quad (\text{E2})$$

$j = x, p$. Introducing, finally, the multimode position and momentum variables

$$u_i \equiv \sum_{j=1}^N (L_x)_{ji} x_j, \quad v_i \equiv \sum_{j=1}^N (L_p)_{ji} p_j, \quad (\text{E3})$$

$i = 1, \dots, N$, and using the formula (E2), we can rewrite the entanglement criterion (E1) into the form

$$\mathcal{U} + \mathcal{V} < \frac{1}{2}, \quad (\text{E4})$$

where we introduced

$$\mathcal{U} \equiv \sum_{i=1}^N \langle (\Delta u_i)^2 \rangle, \quad \mathcal{V} \equiv \sum_{i=1}^N \langle (\Delta v_i)^2 \rangle. \quad (\text{E5})$$

The presented method reveals that the measurement of any block-diagonal witness Z can be realized by a measurement of N linear combinations u_i of position quadratures, and N linear combinations v_i of momentum quadratures, $i = 1, \dots, N$, given in Eq. (E3).

Let us illustrate the general method on a simple two-mode entanglement witness of the form [26]

$$Z = \frac{1}{2(a^2 + \frac{1}{a^2})} \begin{pmatrix} a^2 \mathbb{1} & \frac{|a|}{a} \sigma_z \\ \frac{|a|}{a} \sigma_z & \frac{1}{a^2} \mathbb{1} \end{pmatrix},$$

where $a \in \mathbb{R} \setminus \{0\}$ and σ_z is the Pauli- z matrix, which yields the blocks

$$Z_{x,p} = \frac{1}{2(a^2 + \frac{1}{a^2})} \begin{pmatrix} a^2 & \pm \frac{|a|}{a} \\ \pm \frac{|a|}{a} & \frac{1}{a^2} \end{pmatrix}.$$

The blocks are positive-semidefinite rank-1 matrices and the corresponding lower triangular matrices L_x and L_p are given by

$$L_{x,p} = \frac{1}{\sqrt{2(a^2 + \frac{1}{a^2})}} \begin{pmatrix} |a| & 0 \\ \pm \frac{1}{a} & 0 \end{pmatrix}. \quad (\text{E6})$$

Inserting now the latter matrices into Eq. (E2) and the obtained traces into the inequality (E1), and multiplying the resulting inequality with the nonnegative number $a^2 + \frac{1}{a^2}$ we finally get

$$\langle (\Delta u)^2 \rangle + \langle (\Delta v)^2 \rangle < a^2 + \frac{1}{a^2},$$

where

$$u = |a|x_1 + \frac{1}{a}x_2, \quad v = |a|p_1 - \frac{1}{a}p_2,$$

which is nothing but Duan's *et al.* entanglement criterion [58].

We now apply the previous method to our three-mode partially blind witness of the form \bar{Z}_3 , Eq. (D3). Here and in what follows, we perform the identification $1 \equiv A$, $2 \equiv B$ and $3 \equiv C$. First, let us consider a generic three-mode witness Z for which the matrices Z_x and Z_p are given by

$$Z_j = \begin{pmatrix} (Z_j)_{11} & (Z_j)_{21} & (Z_j)_{31} \\ (Z_j)_{21} & (Z_j)_{22} & (Z_j)_{32} \\ (Z_j)_{31} & (Z_j)_{32} & (Z_j)_{33} \end{pmatrix}. \quad (\text{E7})$$

Restricting ourselves for simplicity to positive-definite matrices $Z_{x,p}$, the lower triangular matrices $L_{x,p}$ appearing in the Cholesky decomposition of the former matrices are then easy to find [50], Sec. 4.2.9] and they are of the form

$$L_j = \begin{pmatrix} (L_j)_{11} & 0 & 0 \\ (L_j)_{21} & (L_j)_{22} & 0 \\ (L_j)_{31} & (L_j)_{32} & (L_j)_{33} \end{pmatrix}, \quad (\text{E8})$$

where

$$\begin{aligned} (L_j)_{11} &= \sqrt{(Z_j)_{11}}, \quad (L_j)_{k1} = \frac{(Z_j)_{k1}}{(L_j)_{11}}, \\ (L_j)_{kk} &= \sqrt{(Z_j)_{kk} - \sum_{l=1}^{k-1} (L_j)_{kl}^2}, \quad k = 2, 3, \\ (L_j)_{32} &= \frac{(Z_j)_{32} - (L_j)_{21}(L_j)_{31}}{(L_j)_{22}}. \end{aligned} \quad (\text{E9})$$

Moving to the partially blind witness \bar{Z}_3 , one further has $(\bar{Z}_{3,x,p})_{31} = 0$, which implies $(L_{x,p})_{31} = 0$ by Eq. (E9) and the matrices (E8) boil down to

$$L_x = \begin{pmatrix} g_1 & 0 & 0 \\ g_2 & g_3 & 0 \\ 0 & g_4 & g_5 \end{pmatrix}, \quad L_p = \begin{pmatrix} h_1 & 0 & 0 \\ h_2 & h_3 & 0 \\ 0 & h_4 & h_5 \end{pmatrix}, \quad (\text{E10})$$

where we set $(L_x)_{11} = g_1$, $(L_x)_{21} = g_2$, $(L_x)_{22} = g_3$, $(L_x)_{32} = g_4$, $(L_x)_{33} = g_5$, $(L_p)_{11} = h_1$, $(L_p)_{21} = h_2$, $(L_p)_{22} = h_3$, $(L_p)_{32} = h_4$, $(L_p)_{33} = h_5$ for brevity. Hence, we get for the variables (E3) the following expressions:

$$\begin{aligned} u_1 &= g_1 x_1 + g_2 x_2, & u_2 &= g_3 x_2 + g_4 x_3, & u_3 &= g_5 x_3, \\ v_1 &= h_1 p_1 + h_2 p_2, & v_2 &= h_3 p_2 + h_4 p_3, & v_3 &= h_5 p_3, \end{aligned} \quad (\text{E11})$$

which then yield

$$\begin{aligned} \mathcal{U} &= \langle [\Delta(g_1 x_1 + g_2 x_2)]^2 \rangle + \langle [\Delta(g_3 x_2 + g_4 x_3)]^2 \rangle \\ &\quad + g_5^2 \langle (\Delta x_3)^2 \rangle, \\ \mathcal{V} &= \langle [\Delta(h_1 p_1 + h_2 p_2)]^2 \rangle + \langle [\Delta(h_3 p_2 + h_4 p_3)]^2 \rangle \\ &\quad + h_5^2 \langle (\Delta p_3)^2 \rangle, \end{aligned} \quad (\text{E12})$$

according to the definition (E5). Substituting into the formulas (E9) for elements of Z the numerical values of the witness \bar{Z}_3 ,

we get

$$\begin{aligned} \{g_1, g_2, g_3, g_4, g_5\} &= \{0.2422, -0.0224, 0.5116, 0.4107, 0.0018\}, \\ \{h_1, h_2, h_3, h_4, h_5\} &= \{0.5806, -0.6821, 0.0754, -0.2482, 0.0092\}. \end{aligned} \quad (\text{E13})$$

This yields for the CM $\bar{\gamma}_3$, Eq. (D2), at the output of the circuit in Fig. 3 the values $\mathcal{U} = 0.2153$ and $\mathcal{V} = 0.2153$, which yields $\mathcal{U} + \mathcal{V} = 0.4306 < 1/2$ and the state with CM $\bar{\gamma}_3$ thus carries genuine multipartite entanglement according to the criterion (E4).

-
- [1] E. Schrödinger, Die gegenwärtige Situation in der Quantenmechanik, *Naturwissenschaften* **23**, 807 (1935); translated in *Quantum Theory and Measurement*, edited by J. A. Wheeler and W. H. Zurek (Princeton University, Princeton, NJ, 1983).
- [2] L. E. Würflinger, J.-D. Bancal, A. Acín, N. Gisin, and T. Vértesi, Nonlocal multipartite correlations from local marginal probabilities, *Phys. Rev. A* **86**, 032117 (2012).
- [3] T. Vértesi, W. Laskowski, and K. F. Pál, Certifying nonlocality from separable marginals, *Phys. Rev. A* **89**, 012115 (2014).
- [4] G. Tóth, Entanglement witnesses in spin models, *Phys. Rev. A* **71**, 010301(R) (2005).
- [5] G. Tóth, C. Knapp, O. Gühne, and H.-J. Briegel, Optimal Spin Squeezing Inequalities Detect Bound Entanglement in Spin Models, *Phys. Rev. Lett.* **99**, 250405 (2007).
- [6] G. Tóth, C. Knapp, O. Gühne, and H.-J. Briegel, Spin squeezing and entanglement, *Phys. Rev. A* **79**, 042334 (2009).
- [7] L. Chen, O. Gittsovich, K. Modi, and M. Piani, Role of correlations in two-body-marginal problem, *Phys. Rev. A* **90**, 042314 (2014).
- [8] N. Miklin, T. Moroder, and O. Gühne, Multiparticle entanglement as an emergent phenomenon, *Phys. Rev. A* **93**, 020104(R) (2016).
- [9] M. Paraschiv, N. Miklin, T. Moroder, and O. Gühne, Proving genuine multiparticle entanglement from separable nearest-neighbor marginals, *Phys. Rev. A* **98**, 062102 (2018).
- [10] W. Dür, J. I. Cirac, and R. Tarrach, Separability and Distillability of Multiparticle Quantum Systems, *Phys. Rev. Lett.* **83**, 3562 (1999).
- [11] D. M. Greenberger, M. Horne, and A. Zeilinger, in *Bell's Theorem, Quantum Theory, and Conceptions of the Universe*, edited by M. Kafatos (Kluwer, Dordrecht, 1989), p. 69.
- [12] L. Amico, R. Fazio, A. Osterloh, and V. Vedral, Entanglement in many-body systems, *Rev. Mod. Phys.* **80**, 517 (2008).
- [13] R. Raussendorf and H. J. Briegel, A One-Way Quantum Computer, *Phys. Rev. Lett.* **86**, 5188 (2001).
- [14] V. Giovannetti, S. Lloyd, and L. Maccone, Quantum-enhanced measurements: Beating the standard quantum limit, *Science* **306**, 1330 (2004).
- [15] P. Horodecki, Separability criterion and inseparable mixed states with positive partial transposition, *Phys. Lett. A* **232**, 333 (1997).
- [16] M. Navascues, F. Baccari, A. Acín, Entanglement marginal problems, *Quantum* **5**, 589 (2021).
- [17] M. Mičuda, R. Stárek, J. Provazník, O. Leskovjanová, and L. Mišta, , Verifying genuine multipartite entanglement of the whole from its separable parts, *Optica* **6**, 896 (2019).
- [18] P. Steinbach, *Field Guide to Simple Graphs* (Design Lab, Albuquerque, 1999), Vol. 3.
- [19] M. Horodecki, P. Horodecki, and R. Horodecki, Separability of mixed states: Necessary and sufficient conditions, *Phys. Lett. A* **223**, 1 (1996).
- [20] B. M. Terhal, Bell inequalities and the separability criterion, *Phys. Lett. A* **271**, 319 (2000).
- [21] L. Vandenberghe and S. Boyd, Semidefinite Programming, *SIAM Rev.* **38**, 49 (1996).
- [22] A. Acín, D. Bruß, M. Lewenstein, and A. Sanpera, Classification of Mixed Three-Qubit States, *Phys. Rev. Lett.* **87**, 040401 (2001).
- [23] M. Bourennane, M. Eibl, Ch. Kurtsiefer, S. Gaertner, H. Weinfurter, O. Gühne, P. Hyllus, D. Bruß, M. Lewenstein, and A. Sanpera, Experimental Detection of Multipartite Entanglement using Witness Operators, *Phys. Rev. Lett.* **92**, 087902 (2004).
- [24] S. L. Braunstein and P. van Loock, Quantum information with continuous variables, *Rev. Mod. Phys.* **77**, 513 (2005).
- [25] Ch. Weedbrook, S. Pirandola, R. García-Patrón, N. J. Cerf, T. C. Ralph, J. H. Shapiro, and S. Lloyd, Gaussian quantum information, *Rev. Mod. Phys.* **84**, 621 (2012).
- [26] P. Hyllus and J. Eisert, Optimal entanglement witnesses for continuous-variable systems, *New J. Phys.* **8**, 51 (2006).
- [27] J. DiGuglielmo, A. Sambrowski, B. Hage, C. Pineda, J. Eisert, and R. Schnabel, Experimental Unconditional Preparation and Detection of a Continuous Bound Entangled State of Light, *Phys. Rev. Lett.* **107**, 240503 (2011).
- [28] R. Simon, Peres-Horodecki Separability Criterion for Continuous Variable Systems, *Phys. Rev. Lett.* **84**, 2726 (2000).
- [29] A. Peres, Separability Criterion for Density Matrices, *Phys. Rev. Lett.* **77**, 1413 (1996).
- [30] R. F. Werner and M. M. Wolf, Bound Entangled Gaussian States, *Phys. Rev. Lett.* **86**, 3658 (2001).
- [31] O. Gühne, P. Hyllus, D. Bruß, A. Ekert, M. Lewenstein, C. Macchiavello, and A. Sanpera, Detection of entanglement with few local measurements, *Phys. Rev. A* **66**, 062305 (2002).
- [32] K. Audenaert and B. De Moor, Optimizing completely positive maps using semidefinite programming, *Phys. Rev. A* **65**, 030302(R) (2002).
- [33] W. Dür and J. I. Cirac, Classification of multiqubit mixed states: Separability and distillability properties, *Phys. Rev. A* **61**, 042314 (2000).
- [34] O. Gühne and G. Tóth, Entanglement detection, *Phys. Rep.* **474**, 1 (2009).
- [35] D. B. West, *Introduction to Graph Theory* (Prentice Hall, Upper Saddle River, 2001).
- [36] OEIS Foundation Inc., The Online Encyclopedia of Integer Sequences, A000055, (2022), <https://oeis.org/A000055>.
- [37] MOSEK ApS, The MOSEK optimization toolbox for MATLAB manual. Version 9.0., <http://docs.mosek.com/9.0/toolbox/index.html> (2019).
- [38] MOSEK ApS, MOSEK Optimizer API for Python manual. Version 9.0, <https://docs.mosek.com/latest/pythonapi/index.html> (2019).

- [39] J. Löfberg, YALMIP A Toolbox for Modeling and Optimization in MATLAB, in *2004 IEEE International Symposium on Computer Aided Control Systems Design, Taipei, Taiwan* (IEEE, 2004).
- [40] G. Sagnol and M. Stahlberg, PICOS: A Python interface to conic optimization solvers, *J. Open Source Software* **7**, 3915 (2022).
- [41] J. Williamson, On the algebraic problem concerning the normal forms of linear dynamical systems, *Am. J. Math.* **58**, 141 (1936).
- [42] S. L. Braunstein, Squeezing as an irreducible resource, *Phys. Rev. A* **71**, 055801 (2005).
- [43] M. Reck, A. Zeilinger, H. J. Bernstein, and P. Bertani, Experimental Realization of Any Discrete Unitary Operator, *Phys. Rev. Lett.* **73**, 58 (1994).
- [44] P. van Loock, Quantum communication with continuous variables, *Fortschr. Phys.* **50**, 1177 (2002).
- [45] G. Vidal and R. F. Werner, Computable measure of entanglement, *Phys. Rev. A* **65**, 032314 (2002).
- [46] A. Serafini, G. Adesso, and F. Illuminati, Unitarily localizable entanglement of Gaussian states, *Phys. Rev. A* **71**, 032349 (2005).
- [47] S. Pirandola, A. Serafini, and S. Lloyd, Correlation matrices of two-mode bosonic systems, *Phys. Rev. A* **79**, 052327 (2009).
- [48] R. A. Horn and C. R. Johnson, *Matrix Analysis* (Cambridge University Press, Cambridge, 1985).
- [49] J. J. Dongarra, J. Bunch, C. Moler, and G. W. Stewart, *LINPACK User's Guide* (SIAM, Philadelphia, 1979).
- [50] G. H. Golub and C. F. Van Loan, *Matrix Computations*, 4th ed. (Johns Hopkins University Press, Baltimore, 1996).
- [51] H. Vahlbruch, M. Mehmet, K. Danzmann, and R. Schnabel, Detection of 15 dB Squeezed States of Light and Their Application for the Absolute Calibration of Photoelectric Quantum Efficiency, *Phys. Rev. Lett.* **117**, 110801 (2016).
- [52] L. K. Shalm, D. R. Hamel, Z. Yan, C. Simon, K. J. Resch, and T. Jennewein, Three-photon energy-time entanglement, *Nat. Phys.* **9**, 19 (2013).
- [53] J. Roslund, R. Medeiros de Araújo, S. Jiang, C. Fabre, and N. Treps, Wavelength-multiplexed quantum networks with ultrafast frequency combs, *Nat. Photonics* **8**, 109 (2014).
- [54] S. Armstrong, M. Wang, R. Y. Teh, Q. Gong, Q. He, J. Janoušek, H.-A. Bachor, M. D. Reid and P. K. Lam, Multipartite Einstein-Podolsky-Rosen steering and genuine tripartite entanglement with optical networks, *Nat. Phys.* **11**, 167 (2015).
- [55] S. Gerke, J. Sperling, W. Vogel, Y. Cai, J. Roslund, N. Treps, and C. Fabre, Full Multipartite Entanglement of Frequency-Comb Gaussian States, *Phys. Rev. Lett.* **114**, 050501 (2015).
- [56] J. Sperling and W. Vogel, Multipartite Entanglement Witnesses, *Phys. Rev. Lett.* **111**, 110503 (2013).
- [57] O. Leskovjanová and L. Mišta, Jr., Classical analog of the quantum marginal problem, *Phys. Rev. A* **101**, 032341 (2020).
- [58] L.-M. Duan, G. Giedke, J. I. Cirac, and P. Zoller, Inseparability Criterion for Continuous Variable Systems, *Phys. Rev. Lett.* **84**, 2722 (2000).